

---

This is an electronic reprint of the original article.  
This reprint may differ from the original in pagination and typographic detail.

Bai, Yunfei; Cui, Kai; Sang, Yushuai; Wu, Kai; Yan, Fei; Mai, Fuhang; Ma, Zewei; Wen, Zhe; Chen, Hong; Chen, Mengmeng; Li, Yongdan

**Catalytic depolymerization of a lignin-rich corncob residue into aromatics in supercritical ethanol over an alumina-supported nimo alloy catalyst**

*Published in:*  
Energy and Fuels

*DOI:*  
[10.1021/acs.energyfuels.9b01457](https://doi.org/10.1021/acs.energyfuels.9b01457)

Published: 19/09/2019

*Document Version*  
Peer-reviewed accepted author manuscript, also known as Final accepted manuscript or Post-print

*Published under the following license:*  
Unspecified

*Please cite the original version:*  
Bai, Y., Cui, K., Sang, Y., Wu, K., Yan, F., Mai, F., Ma, Z., Wen, Z., Chen, H., Chen, M., & Li, Y. (2019). Catalytic depolymerization of a lignin-rich corncob residue into aromatics in supercritical ethanol over an alumina-supported nimo alloy catalyst. *Energy and Fuels*, 33(9), 8657-8665.  
<https://doi.org/10.1021/acs.energyfuels.9b01457>

---

This material is protected by copyright and other intellectual property rights, and duplication or sale of all or part of any of the repository collections is not permitted, except that material may be duplicated by you for your research use or educational purposes in electronic or print form. You must obtain permission for any other use. Electronic or print copies may not be offered, whether for sale or otherwise to anyone who is not an authorised user.

# Catalytic depolymerization of lignin-rich corncob residue into aromatics in supercritical ethanol over an alumina supported NiMo alloy catalyst

Yunfei Bai<sup>a</sup>, Kai Cui<sup>a,b</sup>, Yushuai Sang<sup>a</sup>, Kai Wu<sup>a</sup>, Fei Yan<sup>a</sup>, Fuhang Mai<sup>a</sup>, Zewei Ma<sup>a</sup>, Zhe Wen<sup>a</sup>, Hong Chen<sup>c</sup>, Mengmeng Chen<sup>a\*</sup>, Yongdan Li<sup>a,b\*</sup>

<sup>a</sup> State Key Laboratory of Chemical Engineering (Tianjin University), Tianjin Key Laboratory of Applied Catalysis Science and Technology, School of Chemical Engineering, Tianjin University, Tianjin 300072, China; Collaborative Innovation Center of Chemical Science and Engineering (Tianjin), Tianjin, 300072, China

<sup>b</sup> Department of Chemical and Metallurgical Engineering, Aalto University, Kemistintie 1, FI-00076 Aalto, Finland

<sup>c</sup> School of Environmental Science and Engineering, Tianjin University, Tianjin 300072, China

## Abstract

A one-pot process for the depolymerization of lignin-rich corncob residue (LRCR) is investigated in supercritical ethanol over an alumina supported NiMo (NiMo/Al) alloy catalyst. The LRCR, as a major by-product in corncob enzymatic hydrolysis process, was completely liquefied and effectively transformed into aromatic compounds without the formation of tar or char under optimal reaction condition. Reaction temperature, time, solvent and initial hydrogen pressure have significant effects on the depolymerization of LRCR. The highest overall aromatic yield of 255.4 mg/g LRCR with 57.9 wt % alkylphenols (*e.g.*, 4-ethylphenol, 2,5-diethylphenol and 2,6-diisopropylphenol) was achieved with initial 27.6 bar (gauge) hydrogen in supercritical ethanol at 320 °C for 7.5 h. The depolymerization of LRCR is also examined over Ni/ $\gamma$ -Al<sub>2</sub>O<sub>3</sub>, Mo/ $\gamma$ -Al<sub>2</sub>O<sub>3</sub>, and the physical mixture of these two catalysts. The NiMo/Al alloy catalyst exhibits much higher activity than that of other catalysts, and a synergistic effect between Ni and Mo active species is proposed. Furthermore, XRD results show that Mo<sub>0.24</sub>Ni<sub>0.76</sub> alloy is expected to be an important active species for the depolymerization reaction.

**Keywords:** Lignin, Agricultural waste, NiMo/ $\gamma$ -Al<sub>2</sub>O<sub>3</sub> catalyst, Aromatics, Alkylphenols

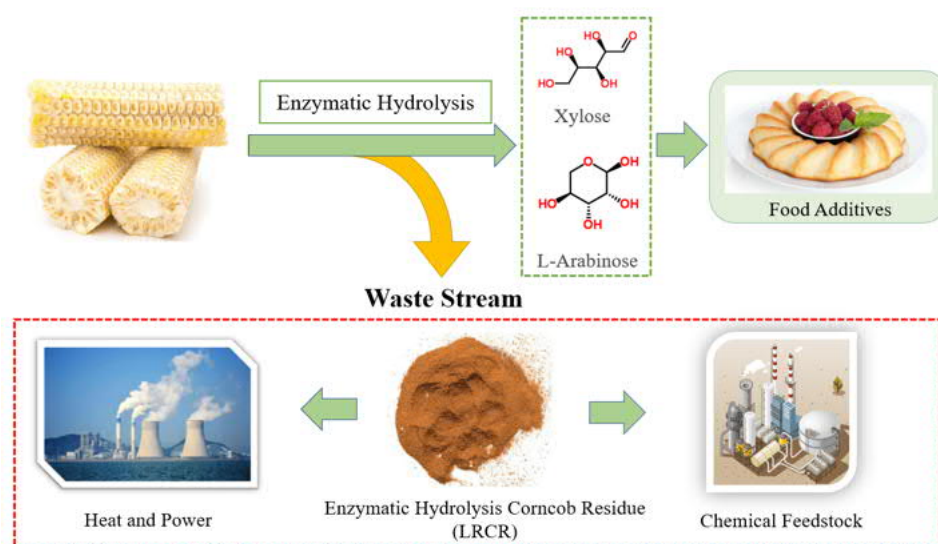
---

\* Corresponding author. E-mail address: mengmeng25@tju.edu.cn (M. Chen).

\* Corresponding author. Tel.: +86 22 27405613; E-mail addresses: yongdan.li@aalto.fi, ydli@tju.edu.cn (Y. Li).

## 1. Introduction

The growing demand for renewable fuels and chemicals has been the continuous driving force for the efficient utilization of biomass.<sup>1</sup> Recently, there has been a great deal of interest for the valorization of non-edible lignocellulose biomass, which primarily consists of cellulose, hemicellulose and lignin.<sup>2,3</sup> As a major component of lignocellulosic biomass, lignin is the most abundant renewable source of aromatic compounds at present.<sup>4,5</sup> Lignin has a macromolecular structure composed of phenyl-propane units linked by C-O-C and C-C bonds, with  $\beta$ -O-4 as the most common linkage.<sup>6-8</sup> Maize is widely planted on earth, and the agricultural waste of corn possesses great potential for the production of fine chemicals.<sup>9</sup> As a major by-product of corncob enzymatic hydrolysis process (Scheme 1), lignin-rich corncob residue (LRCR) is a new type of industrial lignin waste which contains 91.2 wt % of enzymatic hydrolysis lignin. At present, most of LRCR is utilized as low-grade fuel for the generation of heat and power. Therefore, the development of new catalytic technologies for efficient depolymerization of LRCR into aromatics is of great importance.



**Scheme 1.** Comprehensive utilization of waste corncob.

For the depolymerization of lignin, alcoholysis as a process is a novel efficient approach.<sup>10-12</sup> Alcohol in the depolymerization reaction behaves specifically as both the solvent of lignin fragments and the capping agent to stabilize the small molecular products. Therefore, the formation of char is greatly suppressed, and the yields of the target products significantly increase.<sup>13</sup> Ford and co-workers<sup>14</sup> examined the alcoholysis of organosolv lignin in supercritical methanol over a Cu-doped porous metal oxide. The organosolv lignin was effectively converted into cyclohexyl derivatives, and the products have greatly reduced oxygen content. Ethanol solvent also exhibited excellent performance for lignin depolymerization. Ma *et.al.*<sup>15</sup> reported the complete ethanolysis of Kraft lignin over an  $\alpha$ -MoC<sub>1-x</sub>/AC catalyst. The highest overall yield of liquid products, 1.64 g/g lignin, was achieved at 280 °C for 6 h, and no tar or char was detected. Hensen *et.al.*<sup>16</sup> demonstrated a single-step depolymerization process of soda lignin in supercritical ethanol over a CuMgAlO<sub>x</sub> catalyst. A monomer yield of 23 wt % was obtained without char formation at 300 °C for 8 h. Afterwards, Ma *et.al.*<sup>17</sup> proposed that molybdenum(V) ethoxide is the active species for lignin depolymerization over different Mo-based catalysts. In the ethanolysis reaction, ethanol takes the roles of solvent, hydrogen donor as well as a capping agent which suppresses the repolymerization of the lignin-derived phenolic intermediates.<sup>16, 18-20</sup> More critically, as a low toxic and bulk-commercially available chemical, ethanol is an ideal solvent for the industrial application of lignin depolymerization.

Due to the low price and good activity, Ni and Mo based catalysts are widely used in hydrocracking and hydrogenation processes in crude oil refining industry.<sup>21,22</sup> The metallic Ni and Mo catalysts have been also investigated for the depolymerization of lignin and the hydrodeoxygenation (HDO) of bio-oil.<sup>23-25</sup> Song *et.al.*<sup>11</sup> investigated the depolymerization of birch wood lignin over supported Ni metal catalysts, and a lignin conversion of 19% was obtained over a Ni/ $\gamma$ -Al<sub>2</sub>O<sub>3</sub> catalyst in methanol at 200 °C for 6 h. Ma *et.al.*<sup>26</sup> investigated the depolymerization

of Kraft lignin in supercritical ethanol over Mo/ $\gamma$ -Al<sub>2</sub>O<sub>3</sub> catalysts prepared at different reduction temperature. The highest aromatic yield of 332 mg/g lignin was achieved at 280 °C for 6 h over a Mo/ $\gamma$ -Al<sub>2</sub>O<sub>3</sub> catalyst reduced at 750 °C. Recently, Kumar *et.al.*<sup>27</sup> reported a NiMo alloy catalyst which exhibited superior HDO activity for stearic acid, and the conversion of stearic acid was 97.5% at 270 °C for 2 h. C<sub>17-18</sub> alkanes, C<sub>17</sub>-CHO, C<sub>18</sub>-OH were obtained as main product, and the selectivity of alkanes was 48.8%. However, so far, there has been no report for the depolymerization of LRCCR over a NiMo/ $\gamma$ -Al<sub>2</sub>O<sub>3</sub> alloy catalyst in supercritical ethanol.

In this work, a one-pot depolymerization process of LRCCR over an alumina supported NiMo alloy catalyst is reported. The effect of reaction conditions on the LRCCR depolymerization is examined. In addition,  $\gamma$ -Al<sub>2</sub>O<sub>3</sub> support, Ni/ $\gamma$ -Al<sub>2</sub>O<sub>3</sub> (Ni/Al), Mo/ $\gamma$ -Al<sub>2</sub>O<sub>3</sub> (Mo/Al), physical mixture of Ni/Al and Mo/Al and NiMo/ $\gamma$ -Al<sub>2</sub>O<sub>3</sub> (NiMo/Al) alloy catalysts are examined in order to illuminate the synergistic effect between Ni and Mo active species.

## 2. Experimental

### 2.1. Materials

LRCCR was purchased from Shandong Longlive Biotechnology Co. Ltd. The samples were dried at 100 °C for 12 h before use. The LRCCR contains 91.2 wt % lignin, 0.12 wt % residual carbohydrate and 1.42 wt % ash. The weight percentage of C, H, O, N, and S are 61.29, 6.69, 29.61, 0.98, and 0.01 wt % respectively. For the inorganic elements of LRCCR, Cl (0.797 wt %), Na (0.089 wt %), P (0.089 wt %), Fe (0.050 wt %) and Si (0.045 wt %) account for the majority. Hydrogen and nitrogen (99.99%) were supplied by Tianjin Liufang Gas Co. Ltd. Analytical grade chemicals and solvents, including ethanol, methanol and isopropanol were purchased from Tianjin Guangfu Technology Development Co. Ltd. The deionized water was prepared with an Ulupure ultrapure water purification machine (UPH-1-10). Nickel(II) nitrate hexahydrate (Ni(NO<sub>3</sub>)<sub>2</sub>·6H<sub>2</sub>O, 99.9%),

ammonium molybdate tetrahydrate ((NH<sub>4</sub>)<sub>6</sub>Mo<sub>7</sub>O<sub>24</sub>·4H<sub>2</sub>O, 99.98%) and  $\gamma$ -alumina were purchased from Aladdin Co. Ltd and used as received.

## 2.2. Synthesis of catalysts

The  $\gamma$ -alumina was dried at 120 °C for 12 h before use. The monometallic and alloy catalysts were prepared with a successive incipient-wetness impregnation of  $\gamma$ -Al<sub>2</sub>O<sub>3</sub> support with an aqueous solution of ammonium molybdate ((NH<sub>4</sub>)<sub>6</sub>Mo<sub>7</sub>O<sub>24</sub>·4H<sub>2</sub>O) and/or nickel nitrate (Ni(NO<sub>3</sub>)<sub>2</sub>·6H<sub>2</sub>O). The nominal loading of Mo and Ni was 15 wt %. After impregnation, the precursors were dried at 120 °C for 12 h and calcined in air at 500 °C for 12 h. The samples were then heated from 20 to 460 °C at a rate of 5 °C/min and held for 6 h in hydrogen (40 mL/min). All catalysts were used immediately after treatment. The obtained catalysts were named as NiMo/Al, Ni/Al and Mo/Al. For catalyst regeneration experiment, the 2nd used catalyst was calcinated in air at 500 °C for 12 h to remove carbon deposition and reduced at the same conditions.

## 2.3. LRCR depolymerization experiments

The depolymerization reactions were carried out in a 300 mL batch reactor (Parr 4566, made of Hastelloy) equipped with a temperature controller (Parr 4848) and a pressure sensor. In a typical run, 1 g LRCR, 0.5 g catalyst and 50 mL solvent were loaded into the reactor. The reactor was sealed and purged with high-purity nitrogen for six times, then purged with high-purity hydrogen for three times, and finally set at the desired pressure with H<sub>2</sub> and stirred at a rate of 600 rpm. The sealed reactor was heated to reaction temperature and kept for the desired reaction time. After reaction, the liquid products were transferred into a Buser funnel and filtrated to remove solid residues. The solid residues were washed with ethanol and water, dried at 100 °C overnight and then weighed. The liquid products injected neatly into a gas chromatograph-mass spectrometer system (GC-MS, Agilent 6890-5973, HP-5 MS, capillary column, 30 m × 0.25 mm × 0.25  $\mu$ m) for product identification. The oven temperature program for GC and GC-MS was set from an initial

temperature of 45 °C to a final temperature of 250 °C at a rate of 10 °C/min, and kept at 250 °C for 7 min. Afterwards, the products were analyzed and quantified using the internal standard method with a gas chromatograph equipped with a flame ionization detector (GC-FID Agilent 6890, HP-5 MS, capillary column, 30m × 0.25 mm × 0.25 μm) for quantitative analysis. The yield of liquid products was calculated according to the equations:

$$\text{Overall aromatic yield} = \frac{\text{Mass of overall aromatic}}{\text{Dry mass of input LRCR}}$$

$$\text{Alkylphenol yield} = \frac{\text{Mass of alkylphenol}}{\text{Dry mass of input LRCR}}$$

#### 2.4. Characterization

The X-ray powder diffraction (XRD) patterns were collected with the Bruker D8-Focus diffractometer (Cu-K $\alpha$ ,  $\lambda=1.5406 \text{ \AA}$ ) at 40 kV and 40 mA. The powder samples were scanned from 10 to 80 ° at a rate of 10 °/min. The morphology and structure of samples were observed with a scanning electron microscope (SEM: S-4800, JEOL) and a transmission electron microscope (TEM: JEM-2100, HITACHI). Temperature-programmed reduction (TPR) test was performed on the equipment of TP 5080, Tianjin Xianquan. The samples (0.1 g) were placed in a tubular quartz reactor and heated at 40 mL/min flow rate of H<sub>2</sub>/Ar (v:v=1:9) mixture from room temperature to 800 °C with a constant heating rate of 10 °C/min. The hydrogen concentration in the outlet stream during the reduction was measured using a thermal conductivity detector (TCD). Raman spectra of 2nd used catalyst was obtained with a Renishaw inVia reflex spectrometer. Approximately, 50 mg of sample was analyzed under a 633 nm He-Ne laser excitation source.

### 3. Results

#### 3.1. Catalytic activity

##### 3.1.1. Catalytic activity

Figure 1(a) presents the typical total ion chromatogram (TIC) of the liquid products obtained from LRCR depolymerization. The reaction was carried out at 320 °C for 7.5 h, with initial 27.6 bar H<sub>2</sub> in supercritical ethanol over the NiMo/Al catalyst. 17 aromatic compounds were identified and regarded as main products, and the structures of identified molecules are shown in Figure 1(b).

The products are divided into two parts: alkylphenols and other aromatic products.

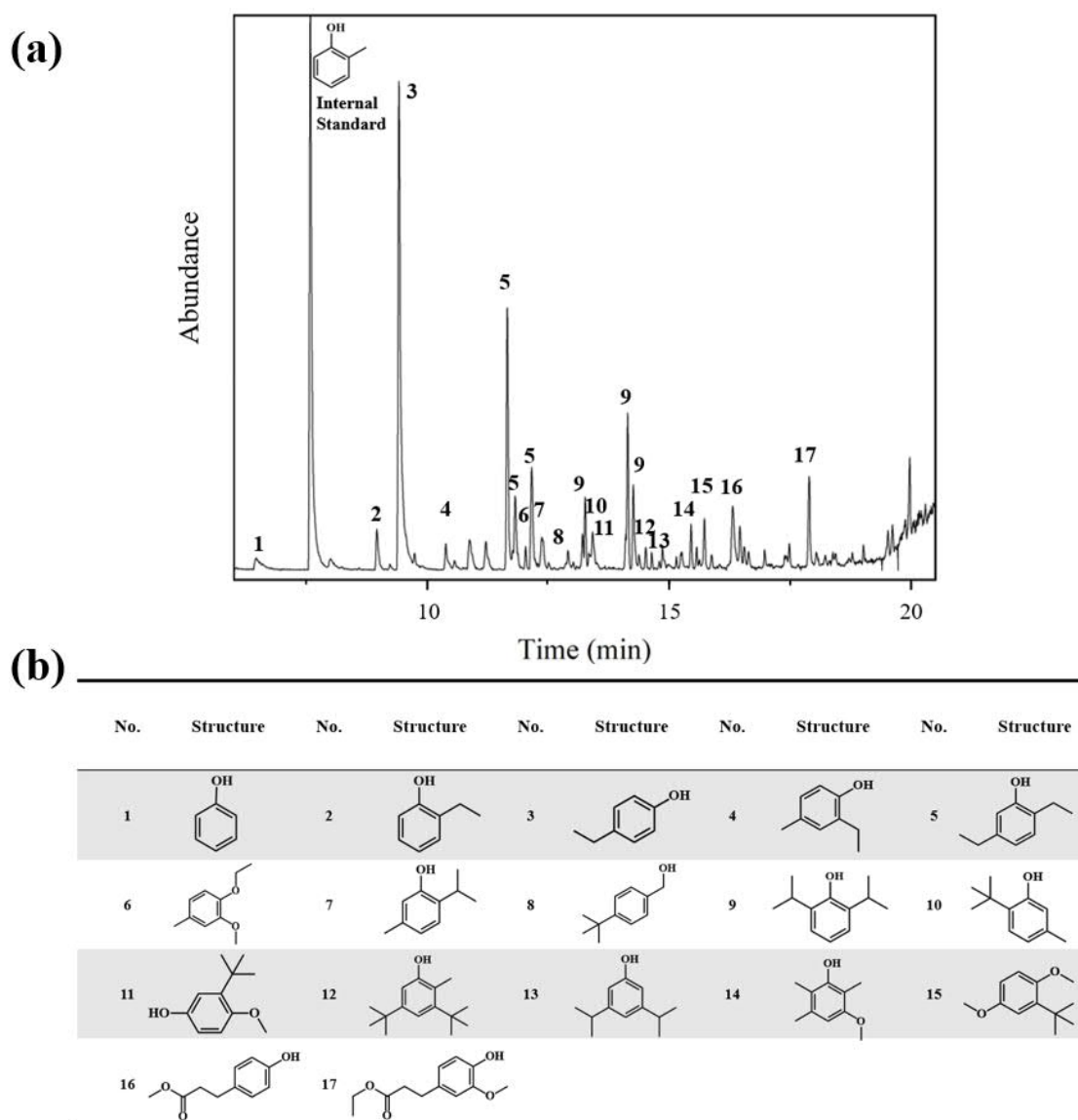


**Figure 1.** a) The TIC of the liquid product obtained from LRCR depolymerization over NiMo/Al; b) Structures of identified molecules in the liquid product.

Note: the numbers in the table are consistent with those in the figure.

Reaction conditions: 320 °C, 27.6 bar H<sub>2</sub>, 7.5 h, 50 mL ethanol.



**Table 1.** The yields of liquid products obtained from LRCR depolymerization over different catalysts.

Entry	Catalyst	Overall Aromatic yield	Alkylphenol yield
		(mg/g LRCR)	(mg/g LRCR)
1	$\gamma$ -Al <sub>2</sub> O <sub>3</sub>	62.4	59.8
2	Ni/Al	102.8	17.7
3	Mo/Al	127.9	120.8
4	Mixture of Mo/Al and Ni/Al	164.7	121.7
5	Fresh NiMo/Al	255.4	147.9
6	1st Used NiMo/Al	158.8	124.4
7	2nd Used NiMo/Al	92.4	48.3

Reaction condition: 320 °C, 27.6 bar H<sub>2</sub>, 7.5 h, 50 mL ethanol.

The comparative experiments were carried out with the  $\gamma$ -Al<sub>2</sub>O<sub>3</sub>, Ni/Al, Mo/Al, physical mixture of Ni/Al and Mo/Al, as well as the fresh and used NiMo/Al catalysts. The results are given in Table 1. With unloaded  $\gamma$ -Al<sub>2</sub>O<sub>3</sub> support as a catalyst, the overall aromatic yield and alkylphenol yield were 62.4 and 59.8 mg/g LRCR, respectively. After reaction, considerable solid residue was observed, which indicates that LRCR was not fully liquified. Compared with unloaded  $\gamma$ -Al<sub>2</sub>O<sub>3</sub>, the overall aromatic yield increased to 102.8 mg/g LRCR with Ni/Al, while the yield of alkylphenols decreased to 17.7 mg/g LRCR. A significantly higher alkylphenol yield (120.8 mg/g LRCR) was obtained over the Mo/Al catalyst, yet the overall aromatic yield (127.9 mg/g LRCR) increased marginally compared to that of the Ni/Al catalyst. In addition, the physical mixture of Ni/Al and Mo/Al gave a higher overall aromatic yield (164.7 mg/g LRCR) and the alkylphenol yield (121.7 mg/g LRCR). Interestingly, the NiMo/Al alloy catalyst exhibited much higher activity. A yield of overall aromatic products, 255.4 mg/g LRCR was obtained over the NiMo/Al catalyst, and the selectivity of the alkylphenols was 57.9 wt %. The overall aromatic product yield increased by 55.1% compared with the physically mixed catalyst. Besides, all LRCR was liquified with no

tar or char formed.

### **3.1.2. Effect of temperature**

The influence of reaction conditions on the yield and distribution of liquid products obtained from LRCR conversion over the NiMo/Al catalyst is illustrated in Figure 2. The effect of reaction temperature on the yields of liquid products was examined over the NiMo/Al catalyst, and the results are illustrated in Figure 2(a). With the reaction temperature increasing from 240 to 320 °C, the overall aromatic yield continued to increase. The highest overall aromatic yield, 255.4 mg/g LRCR, was obtained at 320 °C. For alkylphenol yield and other aromatic yield, the increasing trend was also observed, and the highest yields, 147.9 and 107.5 mg/g LRCR were obtained, respectively, at 320 °C. Moreover, from 280 to 320 °C, the alkylphenol yield shows a larger growth than those of the other aromatic products.

### **3.1.3. Effect of reaction time**

The effect of reaction time on yields of overall aromatic products and alkylphenols over the NiMo/Al catalyst was examined, and the results are plotted in Figure 2(b). From 2.5 to 5 h, the overall aromatic yield increased from 98.1 to 145.3 mg/g LRCR. Meanwhile, the alkylphenol yield increased from 59.2 to 107.4 mg/g LRCR. As the reaction time extended to 7.5 h, the highest overall aromatic yield, 255.4 mg/g LRCR was obtained, with alkylphenol yield of 147.9 mg/g LRCR. As the reaction time further extended to 10 h, the overall aromatic yield decreased to 216.0 mg/g LRCR. However, the alkylphenol yield kept a monotonic increase to 155.1 mg/g LRCR.

### **3.1.4. Effect of initial hydrogen pressure and solvent**

The effect of initial hydrogen pressure was examined, and the results are presented in Figure 2(c). Initial hydrogen pressure tested are 6.9, 13.8 and 27.6 bar. After all the experiments, the weight of the solid residues was less than 0.5 g, and no tar or char was observed in the reactor. With the increase of initial hydrogen pressure, the overall aromatic yield did not change significantly, and

27.6 bar initial hydrogen pressure gave the highest yields of both overall aromatic products (255.4 mg/g LRCR) and alkylphenols (147.9 mg/g LRCR).

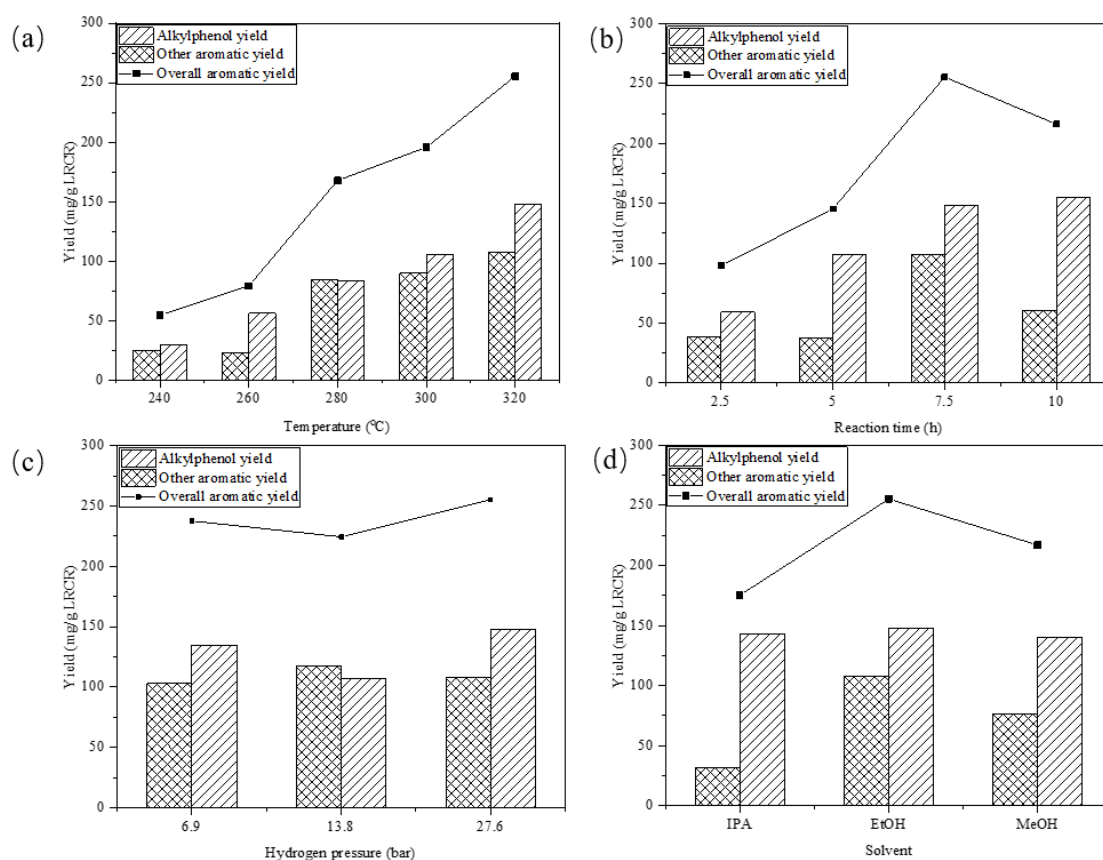


**Figure 2.** The influence of reaction conditions on the yield and distribution of liquid products obtained from LRCR conversion over NiMo/Al catalyst.

(a) Reaction temperature (27.6 bar H<sub>2</sub>, 7.5 h, ethanol); (b) Reaction time (320 °C, 27.6 bar H<sub>2</sub>, ethanol); (c) Hydrogen pressure (320 °C, 7.5 h, ethanol); (d) Solvent (320 °C, 27.6 bar H<sub>2</sub>, 7.5 h).

Furthermore, ethanol (EtOH), methanol (MeOH) and isopropanol (IPA) were tested for LRCR depolymerization over NiMo/Al. The results are shown in Figure 2(d). For alkylphenols, three solvents gave the similar yield of about 140 mg/g LRCR. For the overall aromatic yields, ethanol gave highest yield of 255.4 mg/g LRCR. Methanol and isopropanol exhibited lower activity and gave the overall aromatic yields of 217.0 and 175.3 mg/g LRCR, respectively.

### 3.1.5. Recyclability of the NiMo/Al catalyst

After reaction, the catalyst was readily separated from the liquid products by suction filtration and was directly reused in the successive runs. Figure 3 shows the result of the reusability tests of the catalyst. The yield of overall aromatic products and alkylphenols decreased greatly in the second and third reaction runs. For the third reaction cycle, the yield of overall aromatic products is 92.4 mg/g LRCR and decreased by 63.8% compared with the fresh catalyst. After regeneration, the yields of overall aromatic products and alkylphenols increased to 218.8 and 136.5 mg/g LRCR. The overall yield over regenerated catalyst (REG) decreased by 14.3% compared with fresh NiMo/Al catalyst, and increased by 136.8% compared with the 2nd used catalyst.

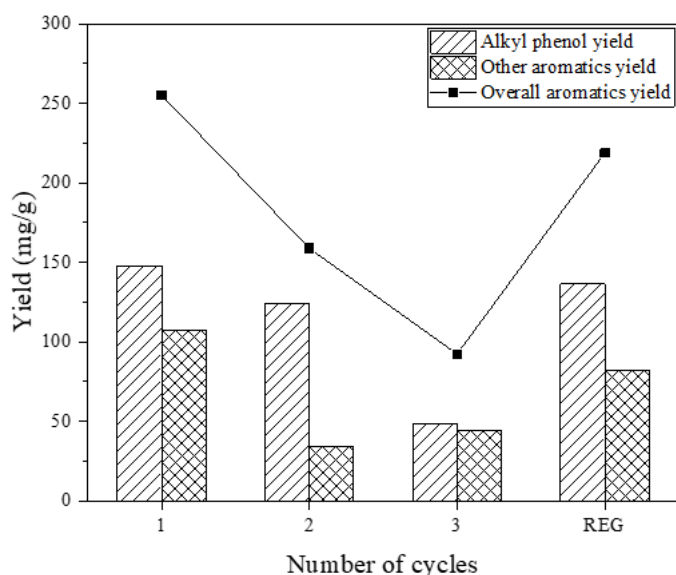


**Figure 3.** The yield and distribution of liquid products obtained from fresh, recycled and regenerated NiMo/Al catalysts.

### 3.2. Catalyst characterization

The XRD patterns of  $\gamma$ -Al<sub>2</sub>O<sub>3</sub> support, Ni/Al, Mo/Al, fresh, 2nd used and regenerated NiMo/Al catalysts are depicted in Figure 4. The diffraction pattern of  $\gamma$ -Al<sub>2</sub>O<sub>3</sub> support shows the clear peaks of Al<sub>2</sub>O<sub>3</sub> (PDF#46-1131), and the same diffraction peaks are also detected in other catalysts and not mentioned below. In the diffraction patterns of Ni/Al and Mo/Al, the peaks of Ni (PDF#04-0850)

and  $\text{MoO}_2$  (PDF#32-0671) are observed respectively. For the fresh NiMo/Al catalyst, the diffraction pattern shows the peaks of  $\text{Mo}_{1.24}\text{Ni}_{0.76}$  (PDF#47-1129), and the peaks of this species are not detected in 2nd used NiMo/Al catalyst. For the regenerated NiMo/Al catalyst, the diffraction peaks of  $\text{Mo}_{1.24}\text{Ni}_{0.76}$  are detected, which verifies the existence of  $\text{Mo}_{1.24}\text{Ni}_{0.76}$ .

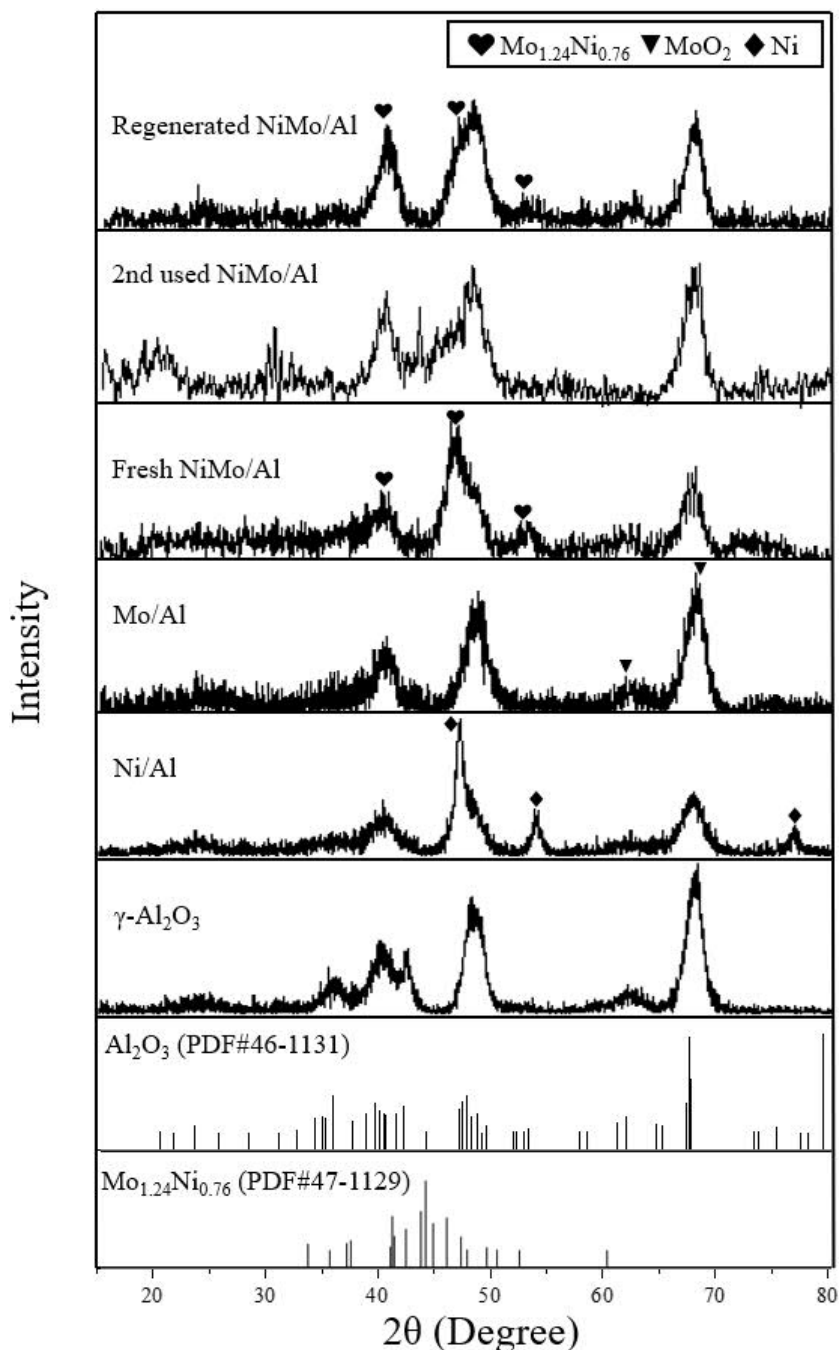


**Figure 4.** XRD patterns of  $\gamma\text{-Al}_2\text{O}_3$  support, Ni/Al, Mo/Al, fresh, 2nd used and regenerated NiMo/Al catalysts.

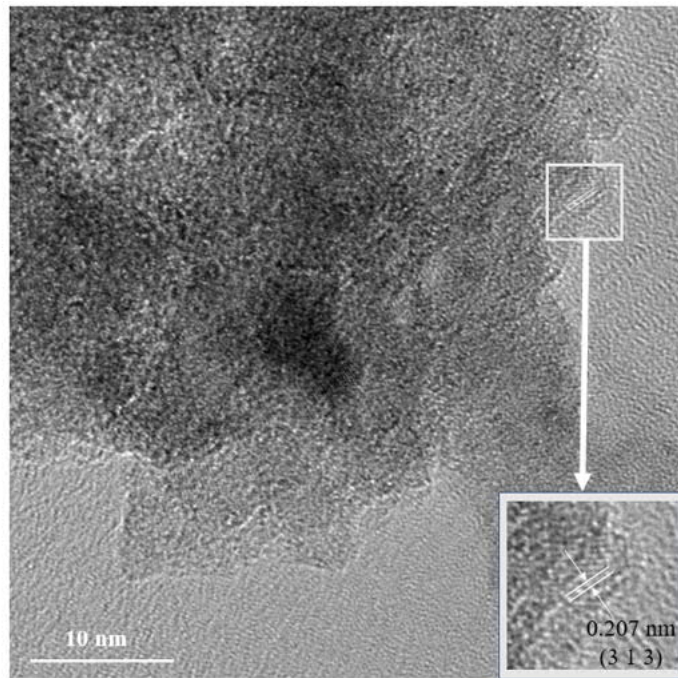


**Figure 5.** High resolution TEM image of fresh NiMo/Al catalyst. The inset is the enlargement of framed area.

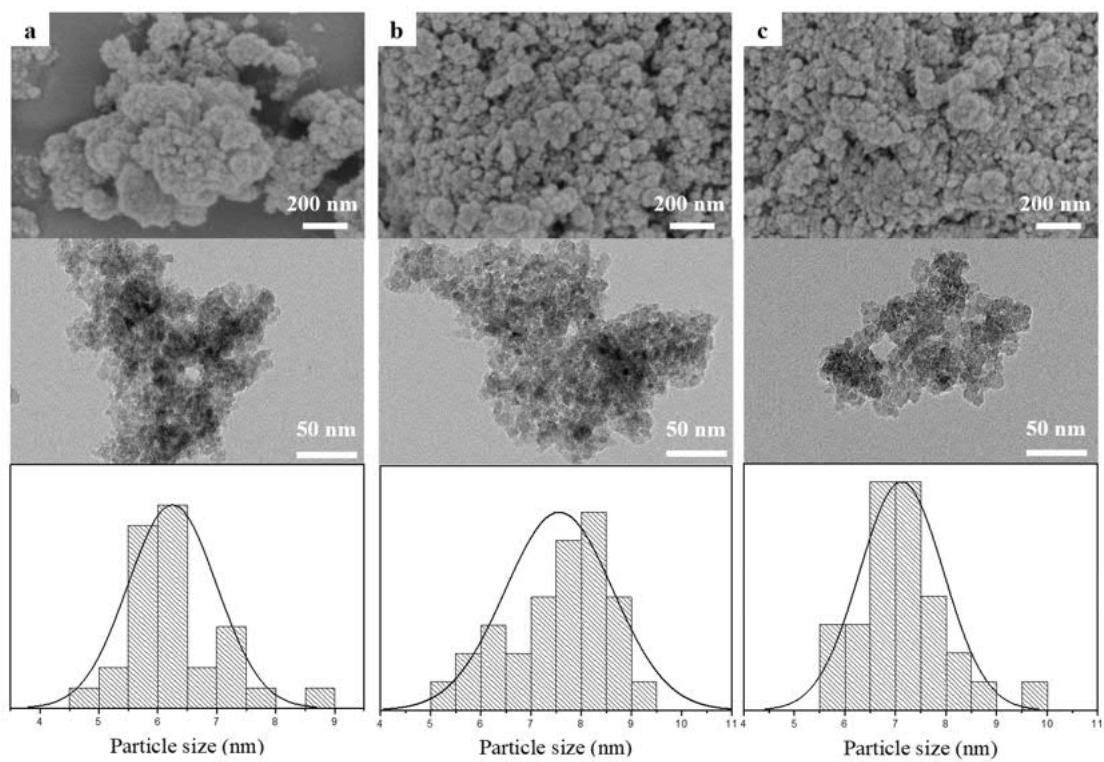


**Figure 6.** SEM (upper), TEM (middle) images and particle size distribution (below) of a)  $\gamma$ -Al<sub>2</sub>O<sub>3</sub> support, b) fresh NiMo/Al catalyst and c) 2nd used NiMo/Al catalyst.

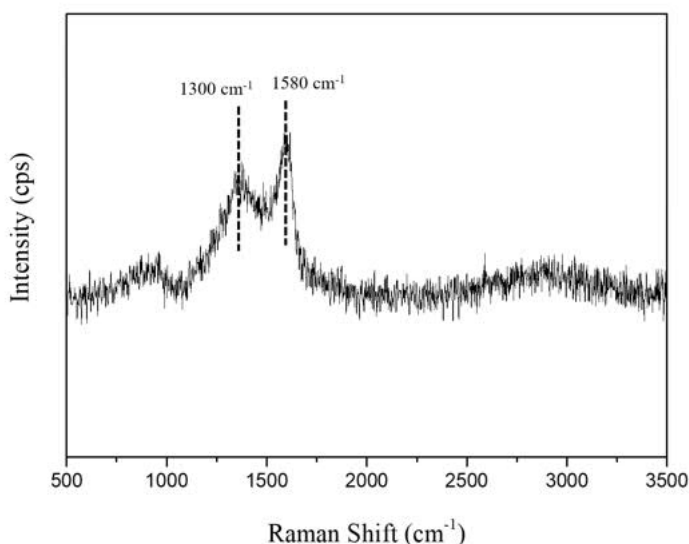


**Figure 7.** Raman spectrum of the 2nd used NiMo/Al catalyst.

High resolution TEM image of the fresh NiMo/Al catalyst is given in Figure 5. The image shows the lattice fringe with a lattice spacing of 0.207 nm, corresponding to that of the (313) face of  $\text{Mo}_{1.24}\text{Ni}_{0.76}$ . Figure 6 displays the SEM and TEM images of the  $\gamma\text{-Al}_2\text{O}_3$ , fresh and 2nd used NiMo/Al catalysts, and the particle size distribution is also exhibited. There is no significant difference among the morphologies of the  $\gamma\text{-Al}_2\text{O}_3$  support, fresh and 2nd used NiMo/Al catalysts. The mean particle diameters of these three catalysts are 6.25, 7.56 and 7.12 nm respectively, implying that the structure and particle size of  $\gamma\text{-Al}_2\text{O}_3$  support is stable during catalyst synthesis and reaction process. The Raman spectra of the 2nd used NiMo/Al catalyst is given in Figure 7, the peaks at 1300 and 1580  $\text{cm}^{-1}$  are associated with the characteristic peaks of amorphous and graphite carbon respectively.

TPR profiles for the NiMo/Al, Ni/Al and Mo/Al catalysts are presented in Figure 8. For the monometallic Ni/Al catalyst, three main peaks occur. A small reduction peak at about 390 °C is attributed to reduction of the well-crystallized NiO species.<sup>23</sup> A larger reduction peak at about 520 °C is attributed to the reduction of oxidized Ni species strongly interacting with the  $\gamma\text{-Al}_2\text{O}_3$  support. The broad peak at 740 °C is associated with the hardly reducible nickel aluminate. The

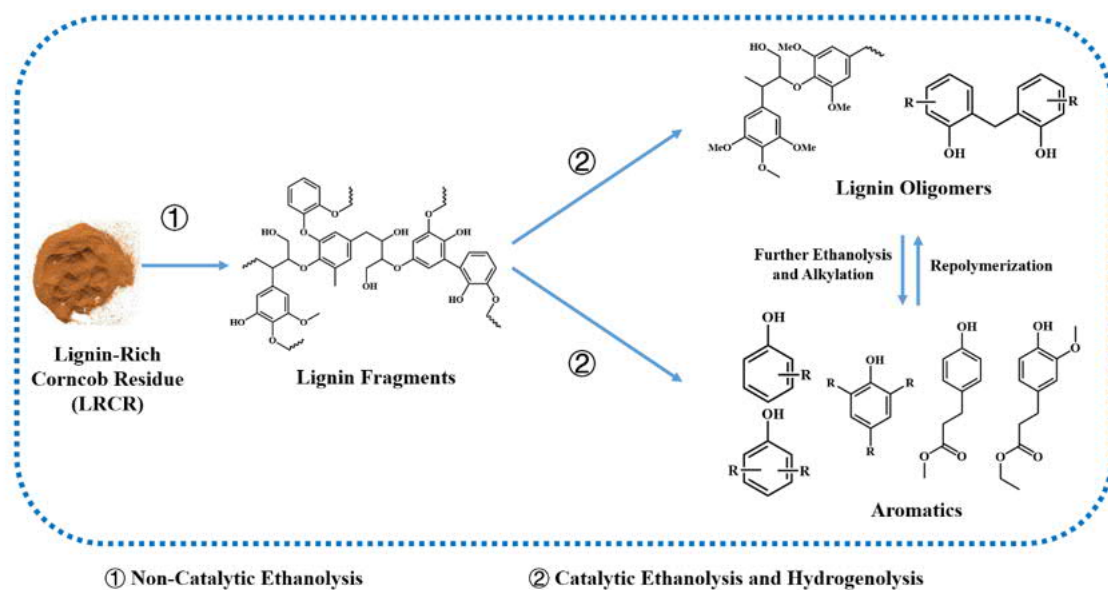
TPR curve of Mo/Al exhibits two large peaks at 460 and 760 °C, and they are caused by the reductions of MoO<sub>3</sub> to MoO<sub>2</sub> and MoO<sub>2</sub> to Mo, respectively.<sup>24</sup> For the NiMo/Al catalyst, three hydrogen consumption peaks at 410 °C, 470 °C and 750 °C occur. Yin *et al.*<sup>22</sup> proposed that the hydrogen consumption region from 350 to 650 °C was associated with the reduction of Mo<sup>6+</sup> to Mo<sup>4+</sup> and Mo<sup>0</sup>, and the reduction of Ni<sup>2+</sup> to Ni<sup>0</sup>. The reduction peak at 750 °C is associated with the reduction of the remaining Mo<sup>4+</sup> to Mo<sup>0</sup> and the reduction of nickel aluminate.

#### 4. Discussion

Due to the low ash content and high lignin purity, LRCR can be directly utilized without any chemical pretreatment. The catalytic depolymerization of LRCR probably happened as shown in Scheme 2. At first, LRCR underwent a noncatalytic ethanolysis step, resulting in the formation of lignin fragments and a small amount of monomers. In the second step, the complete depolymerization of these fragments into monomers catalyzed by Ni and Mo active species was achieved, accompanied by HDO and alkylation reactions. Hartwig *et al.*<sup>28</sup> proved that the nickel-based catalyst is effective for the hydrogenolysis of C-O bonds in lignin. However, the monometallic Ni/Al catalyst failed to give high overall aromatic yield, and the alkylphenol yield was only 17.7 mg/g LRCR, which is likely attributed to the low alkylation activity of Ni species. For the depolymerization of LRCR, Huang *et al.*<sup>29</sup> proposed that the alkylation plays an important role on suppressing lignin monomers repolymerization. A good correlation between the extent of polymerization and the degree of monomer alkylation is observed, and the monomers with alkyl substitutes at ortho- and para-positions present low repolymerization tendency. Besides, the alkylation reaction at meta-position prevents the formation of repolymerization-active phenolic hydroxyl group.<sup>30</sup> A considerable alkylphenol yield of 120.8 mg/g LRCR was obtained due to the good activity of the Mo/Al catalyst towards the alkylation reaction, as reported in our previous



work.<sup>16,24</sup> Hence, the catalytic role of the Mo species in the NiMo/Al catalyst is supposed to prevent the lignin monomers from repolymerization.



**Scheme 2.** Possible reaction pathway for LRCR depolymerization.

For comparative experiments of the monometallic and alloy catalysts, NiMo/Al exhibited much higher activity than Ni/Al and Mo/Al. The overall aromatic yield obtained over the NiMo/Al catalyst is even higher than the sum of the yields obtained over Ni/Al and Mo/Al under otherwise the same reaction conditions. Additionally, the physical mixture of Ni/Al and Mo/Al also exhibited lower activity than the NiMo/Al catalyst. Hence, the Ni and Mo active species in the NiMo/Al catalyst are supposed to have a synergistic effect, which leads to the high activity for LRCR depolymerization. Interestingly, a remarkable relevance between the overall aromatic yield and the XRD intensity of  $\text{Mo}_{1.24}\text{Ni}_{0.76}$  phase is observed. After two successive reaction cycles, the diffraction peaks of  $\text{Mo}_{1.24}\text{Ni}_{0.76}$  disappeared, and the overall aromatic yield dropped dramatically to 92.4 mg/g LRCR. Compared to the fresh NiMo/Al catalyst, the 2nd used NiMo/Al catalyst exhibited much lower activity, indicating that  $\text{Mo}_{1.24}\text{Ni}_{0.76}$  is an important active species for LRCR depolymerization. Moreover, Raman spectrum analysis verifies that both amorphous and graphite

carbon exist on the surface of the 2nd used catalyst. Hence, it can be concluded that the deactivation of NiMo/Al is mainly caused by the disappearance of the NiMo alloy and the deposition of carbon. In catalyst recycle experiments, the activity of regenerated NiMo/Al catalyst increased greatly compared to the 2nd used catalyst. In addition, the XRD pattern of regenerated catalyst demonstrates that the  $\text{Mo}_{1.24}\text{Ni}_{0.76}$  active species was regenerated in the calcination-reduction process.

Reaction conditions also have significant influence on both overall aromatic and alkylphenol yields. With the reaction temperature increasing from 240 to 320 °C, the increase of overall aromatic and alkylphenol yield is likely ascribed to the better lignin solubility as well as the faster depolymerization reaction rate. From 280 to 320 °C, the alkylphenol yield shows a larger growth than that of other aromatic products, demonstrating that high temperature also plays a critical role on the subsequent alkylation reaction. According to the previous work, elevated temperature favors higher overall aromatic yield, because it is conducive to the formation of radicals from ethanol, thus facilitating the depolymerization of lignin.<sup>16,18</sup> With reaction time prolonging from 2.5 to 7.5 h, the depolymerization of lignin fragments was the predominant reaction in the process, leading to the increase of overall aromatic yield. For longer reaction time, the reaction rate of repolymerization exceeded that of depolymerization, resulting in the decrease of the overall aromatic yield. However, the alkylphenol yield continued to increase with reaction time prolonging. It indicates that the alkylation reaction continually proceeded, resulting in the transformation of monomers into alkylphenols. During the depolymerization process of LRCR, monomers were formed and underwent further alkylation reaction, producing alkylphenol products and restraining repolymerization.

For the depolymerization of LRCR, hydrogenolysis is an important process which facilitates the formation of aromatic monomers. To enhance the effective hydrogenolysis of LRCR, active H

species from solvent or gaseous hydrogen is required. Therefore, both hydrogen atmosphere and alcohol solvent are employed in our research. For overall aromatic yield, solvent type shows a remarkable influence, which is in accordance with previous results.<sup>14,31</sup> Additionally, in lignin depolymerization process, hydrogen pressure enhanced the HDO rate and inhibited char formation. The role of H species is expected to stabilize the radicals formed during depolymerization, which prevented their repolymerization.<sup>32</sup> Ma *et.al.*<sup>16</sup> investigated the effect of ethanol solvent on Kraft lignin ethanolysis. According to their result, ethanol solvent helps to form dissociative Mo active species, and played important roles in stabilizing monomers as well as suppressing the repolymerization of the primary products. With the good performance of ethanol solvent and remarkable activity of the  $\text{Mo}_{1.24}\text{Ni}_{0.76}$  species, LRCR is effectively depolymerized over the NiMo/Al catalyst, and high aromatic yield is obtained. Moreover, the one-pot process is easy-operating, low-cost and the catalyst is readily recycled and regenerated. Considering the economic and environmental benefits, this one-pot depolymerization process of LRCR has good prospect for future practical application.

## 5. Conclusions

LRCR was completely liquified and depolymerized to aromatic compounds with considerable yield over a NiMo/Al alloy catalyst. The highest overall aromatic yield, 255.4 mg/g LRCR, is achieved at 320 °C for 7.5 h under 27.6 bar hydrogen pressure in supercritical ethanol, and the alkylphenol yield is 147.9 mg/g LRCR. High temperature and ethanol solvent facilitate the LRCR depolymerization. Moreover, the Ni/Al, Mo/Al and the physical mixture of Ni/Al and Mo/Al catalysts exhibited much lower activity than the NiMo/Al alloy catalyst. The catalytic activity is strongly related to the existence of  $\text{Mo}_{1.24}\text{Ni}_{0.76}$ , suggesting that  $\text{Mo}_{1.24}\text{Ni}_{0.76}$  is an important active species in the reaction.

## Acknowledgements

Financial support from the Natural Science Foundation of China under Contracts 21336008 and 21690083 and the Ministry of Science and Technology of China under contract 2011DFA41000 is gratefully acknowledged. This research was also supported in part by the Program of Introducing Talents to the University Disciplines under File No. B06006 and the Program for Changjiang Scholars and Innovative Research Teams in Universities under File No. IRT 0641.

## References

- (1) Dapsens, P. Y.; Mondelli, C.; Pérez-Ramírez, J. Biobased Chemicals from Conception toward Industrial Reality: Lessons Learned and to Be Learned. *ACS Catal.* **2012**, *2* (7), 1487-1499.
- (2) Sjöström, E. *Wood Chemistry: Fundamentals and Applications*. Academic Press: New York, 1981.
- (3) Li, C., Zhao, X., Wang, A., Huber, G. W., Zhang, T. Catalytic Transformation of Lignin for the Production of Chemicals and Fuels. *Chem. Rev.* **2015**, *115* (21), 11559-11624.
- (4) Azadi, P., Inderwildi, O. R., Farnood, R., King, D. A. Liquid Fuels, Hydrogen and Chemicals from Lignin: A Critical Review. *Renew. Sust. Energ. Rev.* **2013**, *21* (5), 506-523.
- (5) Ragauskas, A.; Beckham, G.; Biddy, M.; Richard, C.; Fang, C.; Davis, M.; Davison, B.; Dixon, R.; Paul, G.; Martin, K. Lignin Valorization: Improving Lignin Processing in the Biorefinery. *Science.* **2014**, *344* (6185), 1246843-1246843.
- (6) Stöcker, M. Biofuels and Biomass-to-Liquid Fuels in the Biorefinery: Catalytic Conversion of Lignocellulosic Biomass Using Porous Materials. *Angew. Chem. Int. Ed.* **2008**, *47* (48), 9200-9211.
- (7) Zakzeski, J.; Bruijninx, P. C. A.; Jongerius, A. L.; Weckhuysen, B. M. The Catalytic Valorization of Lignin for the Production of Renewable Chemicals. *Chem. Rev.* **2010**, *110* (6),

3552-3599.

(8) Vom Stein, T.; Den Hartog, T.; Buendia, J.; Stoychev, S.; Mottweiler, J.; Bolm, C.; Klankermayer, J.; Leitner, W. Ruthenium-Catalyzed C-C Bond Cleavage in Lignin Model Substrates. *Angew. Chem. Int. Ed.* **2015**, *54* (20), 5859-5863.

(9) Song, S.; Zhang, J.; Yan, N. Production of Terephthalic Acid from Corn Stover Lignin. *Angew. Chem. Int. Ed.* **2019**, *58*, 4934-4937.

(10) Warner, G.; Hansen, T. S.; Riisager, A.; Beach, E. S.; Barta, K.; Anastas, P. T. Depolymerization of Organosolv Lignin Using Doped Porous Metal Oxides in Supercritical Methanol. *Bioresour. Technol.* **2014**, *161*, 78-83.

(11) Song, Q.; Wang, F.; Cai, J.; Wang, Y.; Zhang, J.; Yu, W.; Xu, J. Lignin Depolymerization (LDP) in Alcohol over Nickel-Based Catalysts via a Fragmentation-Hydrogenolysis Process. *Energy Environ. Sci.* **2013**, *6* (3), 994-1007.

(12) Ferrini, P.; Rinaldi, R. Catalytic Biorefining of Plant Biomass to Non-Pyrolytic Lignin Bio-Oil and Carbohydrates through Hydrogen Transfer Reactions. *Angew. Chem. Int. Ed.* **2014**, *53* (33), 8634-8639.

(13) Zhu, S.; Guo, J.; Wang, X.; Wang, J.; Fan, W. Alcoholysis: A Promising Technology for Conversion of Lignocellulose and Platform Chemicals. *ChemSusChem* **2017**, *10* (12), 2547-2559.

(14) Barta, K.; Matson, T. D.; Fettig, M. L.; Scott, S. L.; Iretskii, A. V.; Ford, P. C. Catalytic Disassembly of an Organosolv Lignin via Hydrogen Transfer from Supercritical Methanol. *Green Chem.* **2010**, *12* (9), 1640-1647.

(15) Ma, R.; Hao, W.; Ma, X.; Tian, Y.; Li, Y. Catalytic Ethanolysis of Kraft Lignin into High-Value Small-Molecular Chemicals over a Nanostructured  $\alpha$ -Molybdenum Carbide Catalyst. *Angew. Chem. Int. Ed.* **2014**, *53* (28), 7310-7315.

(16) Huang, X.; Korányi, T. I.; Boot, M. D.; Hensen, E. J. M. Catalytic Depolymerization of Lignin

in Supercritical Ethanol. *ChemSusChem* **2014**, 7 (8), 2276-2288.

(17) Ma, X.; Ma, R.; Hao, W.; Chen, M.; Yan, F.; Cui, K.; Tian, Y.; Li, Y. Common Pathways in Ethanolysis of Kraft Lignin to Platform Chemicals over Molybdenum-Based Catalysts. *ACS Catal.* **2015**, 5 (8), 4803-4813.

(18) Voitl, T.; Von Rohr, P. R. Oxidation of Lignin Using Aqueous Polyoxometalates in the Presence of Alcohols. *ChemSusChem* **2008**, 1 (8-9), 763-769.

(19) Onwudili, J. A. Influence of Reaction Conditions on the Composition of Liquid Products from Two-Stage Catalytic Hydrothermal Processing of Lignin. *Bioresour. Technol.* **2015**, 187, 60-69.

(20) Deuss, P. J.; Scott, M.; Tran, F.; Westwood, N. J.; De Vries, J. G.; Barta, K. Aromatic Monomers by in Situ Conversion of Reactive Intermediates in the Acid-Catalyzed Depolymerization of Lignin. *J. Am. Chem. Soc.* **2015**, 137 (23), 7456-7467.

(21) Ward J. Hydrocracking Processes and Catalysts. *Fuel Process. Technol.* **1993**, 35(1), 55-85.

(22) Furimsky, E. Catalytic Hydrodeoxygenation. *Appl. Catal., B* **2000**, 199 (2), 147-190.

(23) Oregui-Bengoechea, M.; Gandarias, I.; Miletić, N.; Simonsen, S. F.; Kronstad, A.; Arias, P. L.; Barth, T. Thermocatalytic Conversion of Lignin in an Ethanol/Formic Acid Medium with NiMo Catalysts: Role of the Metal and Acid Sites. *Appl. Catal., B* **2017**, 217, 353-364.

(24) Yin, W.; Venderbosch, R. H.; He, S.; Bykova, M. V.; Khromova, S. A.; Yakovlev, V. A.; Heeres, H. J. Mono-, Bi-, and Tri-Metallic Ni-Based Catalysts for the Catalytic Hydrotreatment of Pyrolysis Liquids. *Biomass Convers. Biorefinery* **2017**, 7 (3), 361-376.

(25) Sudipta, D.; Zhang, J.; Luque, R.; Yan, N. Ni-based bimetallic heterogeneous catalysts for energy and environmental applications. *Energy Environ. Sci.* **2016**, 9, 3314-3347.

(26) Ma, X.; Cui, K.; Hao, W.; Ma, R.; Tian, Y.; Li, Y. Alumina Supported Molybdenum Catalyst for Lignin Valorization: Effect of Reduction Temperature. *Bioresour. Technol.* **2015**, 192, 17-22.

(27) Kumar, P.; Maity, S. K.; Shee, D. Role of NiMo Alloy and Ni Species in the Performance of

- NiMo/Alumina Catalysts for Hydrodeoxygenation of Stearic Acid: A Kinetic Study. *ACS Omega* **2019**, *4* (2), 2833-2843.
- (28) Gao, F.; Webb, J. D.; Hartwig, J. F. Chemo- and Regioselective Hydrogenolysis of Diaryl Ether C-O Bonds by a Robust Heterogeneous Ni/C Catalyst: Applications to the Cleavage of Complex Lignin-Related Fragments. *Angew. Chem. Int. Ed.* **2016**, *55* (4), 1474-1478.
- (29) Huang, X.; Korányi, T.; Boot, D.; Hensen, E. Ethanol as Capping Agent and Formaldehyde Scavenger for Efficient Depolymerization of Lignin to Aromatics. *Green Chem.* **2015**, *17* (11), 4941-4950.
- (30) Li, S.; Basudeb, S. Towards high-yield lignin monomer production. *Green Chem.* **2017**, *19* (16), 3752-3758.
- (31) Yuan, Z.; Tymchyshyn, M.; Xu, C. Reductive Depolymerization of Kraft and Organosolv Lignin in Supercritical Acetone for Chemicals and Materials. *ChemCatChem* **2016**, *8* (11), 1968-1976.
- (32) Grilc, M.; Likozar, B.; Levec, J. Simultaneous Liquefaction and Hydrodeoxygenation of Lignocellulosic Biomass over NiMo/Al<sub>2</sub>O<sub>3</sub>, Pd/Al<sub>2</sub>O<sub>3</sub>, and Zeolite Y Catalysts in Hydrogen Donor Solvents. *ChemCatChem* **2016**, *8* (1), 180-191.